

# CORRECTION OF THE MAGNETIC FIELD IN THE NICA COLLIDER

O. Kozlov, A. Butenko, S. Kostromin, I. Meshkov, A. Sidorin, E. Syresin, JINR, Dubna, Russia

## Abstract

The magnetic field correction systems in the optimized lattice of the NICA collider are considered. The dipole, normal and skew quadrupoles, sextupole and octupole additional windings are placed in the corrector elements to compensate separately the alignment errors, betatron tune shifts, betatron coupling, chromaticity and non-linear fields. The overall correction effect should increase the dynamic aperture and provide the required beam and luminosity lifetime of the collider.

## INTRODUCTION

The Nuclotron-based Ion Collider fAcility (NICA) [1] is a new accelerator complex being constructed at JINR. Two collider rings are designed and optimized to achieve the required luminosity at two interaction points (IP). The first IP is connected with Multipurpose detector (MPD) for the ion-ion ( $Au^{+79}$ ) collider experiments in the energy range of  $1 \div 4.5$  GeV/u. The second IP is aimed for the polarized proton-proton ( $5 \div 12.6$  GeV) and deuteron-deuteron ( $2 \div 5.8$  GeV/u) collisions. The collider lattice is based on the technology of super-ferric magnets developed in VBLHE, JINR. The collider optics is optimized to obtain the required luminosity (Table 1) with the certain effects which set constraints on the lattice parameters: luminosity lifetime limitation by intrabeam scattering in a bunch (IBS), space charge tune shift, threshold of microwave instability, slippage factor optimization for efficient stochastic cooling, maximum required RF voltage amplitude. This paper considers the  $^{197}Au^{+79}$  heavy ion mode of facility operation. The possible schemes of the correction of the linear and non-linear imperfections of the magnetic fields of the structural elements of the collider are supplied to the collider optics to increase the dynamic aperture.

## LATTICE OF THE RINGS

Collider lattice was developed and optimized [2] with some constraints: ring circumference, a number of the dipole magnets in an arc, convenience of the beam injection into the ring. The rings are vertically separated (32 cm between axes) and use two-aperture superconducting magnets (dipoles and quadrupoles). Rings have the racetrack shape with the bending arcs and long straight section. The principal choice for the arc structure is the FODO optics with 12 periods. Circumference of the rings corresponds exactly to two Nuclotron circumferences. The project parameters of the collider ring are presented in Table 1.

Bending arc comprises 12 FODO cells with nominal

Table 1: Project Parameters of the Collider Rings

Ring circumference, m	503.04		
Number of bunches	22		
Rms bunch length, m	0.6		
$\beta$ -function in the IP, m	0.35		
Betatron tunes, $Q_x/Q_y$	9.44/9.44		
Chromaticity, $Q'_{x,0}/Q'_{y,0}$	-33/-28		
Acceptance $\pi \cdot \text{mm} \cdot \text{mrad}$	40		
Long. acceptance, $\Delta p/p$	$\pm 0.010$		
Gamma-transition, $\gamma_{tr}$	7.088		
Ion energy, GeV/u	1.0	3.0	4.5
Ion number per bunch	$2.0 \cdot 10^8$	$2.4 \cdot 10^9$	$2.3 \cdot 10^9$
Rms $\Delta p/p$ , $10^{-3}$	0.55	1.15	1.50
Rms emittance, hor./vert. (unnorm.), $\pi \cdot \text{mm} \cdot \text{mrad}$	1.10/ 0.95	1.10/ 0.85	1.10/ 0.75
Luminosity, $\text{cm}^{-2} \cdot \text{s}^{-1}$	$0.6 \cdot 10^{25}$	$1.0 \cdot 10^{27}$	$1.0 \cdot 10^{27}$
IBS growth time, s	170	470	2000
Tune shift, $\Delta Q_{SC} + 2\Delta Q_{bb}$	-0.050	-0.037	-0.011

betatron phase advances of  $90^\circ$  per cell. The cells with empty dipoles are used for horizontal dispersion suppression and convenient beam injection and extraction (dumping) schemes. Periodic FODO cell consists of four rectangular dipole magnets per cell (80 magnets per ring), two quadrupoles [3], multipole correctors and beam position monitors (BPM) (Fig. 1). The maximum field in 1.94 m dipole of 1.8 T and gradient in 0.47 m quadrupoles of 23 T/m. The long straight sections matched to the arcs contain the RF stations, electron and stochastic cooling devices, BPMs, superconducting quadrupole blocks. The optics in these sections produces the betatron tune variation, vertical beam separation in the rings and conditions for colliding beams in interaction points (IP). The schematic composition of the rings is given in Fig. 2. The Twiss-functions of the ring are shown in Fig. 3.

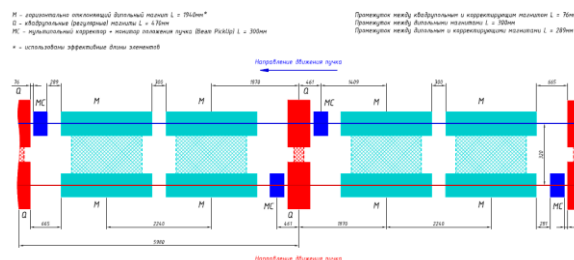


Figure 1: Periodic FODO cells for both rings.

Content from this work may be used under the terms of the CC BY 3.0 licence (© 2018). Any distribution of this work must maintain attribution to the author(s), title of the work, publisher, and DOI.

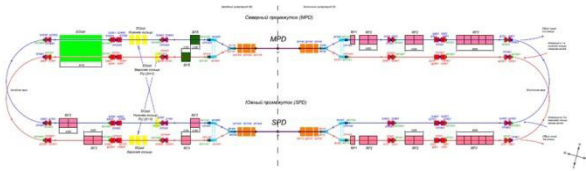


Figure 2: Collider scheme and equipment layout.

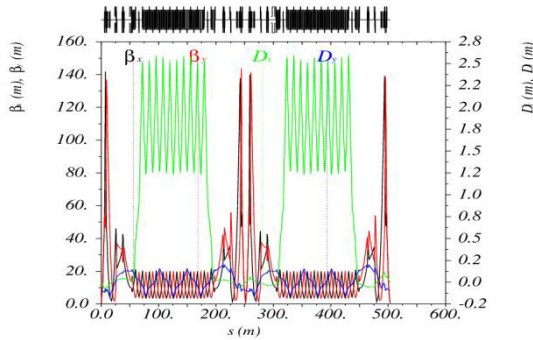


Figure 3: Collider Twiss-functions,  $\beta = 0.60$  m.

### CORRECTION OF MAGNETIC FIELD

For the stable circulation of the ion beam in the collider the definite magnetic field correction systems should be provided in the collider optical structure. The following required set of correcting circuits are considered for the collider rings: correction of the closed orbit distortions, linear betatron tune shift correction, correction of the transversal betatron oscillations coupling, compensation of the vertical dispersion, correction of the chromaticity of the betatron tunes, higher order non-linear effects compensation including fringe field effect. Multipole corrector element is designed for these purposes. It has the length of 0.3 m and up to the four layers of the “cosine-type” superconducting windings. The multipole correctors are located next to the superconducting quadrupoles in the arcs and in the straight section. The required maximal number and maximal strength of the correcting winding are obtained from the beam dynamics calculation.

Dipole closed orbit correction parameters are defined from the numerical statistical experiment by the calculation the number of the random closed orbits caused by the following sources of distortions (r.m.s. values):  $\sigma_{\Delta B/B} = 5 \cdot 10^{-4}$ ,  $\sigma_{\Delta s} = 0.5$  mm,  $\sigma_{\Delta y} = 0.5$  mm,  $\sigma_{\Delta \phi} = 0.5$  mrad – spread of the guiding field, longitudinal shift, vertical shift, roll angle in dipole magnets;  $\sigma_{\Delta x/\Delta x} = 0.1$  mm – transversal shifts of the quadrupole axes. Then the maximal excursions of the 100 closed orbits are obtained. The correction algorithm (MICADO [3]) is applied for each orbit with the additional requirements for residual orbit ( $\sigma_{x/y} = 0.1$  mm), maximal number of the used corrector ( $n_{corr} = 30 \div 50$ ) and the maximal correction angle kick ( $\theta_{corr} \approx 0.01 \cdot \theta_{dip}$ ). As a result of these calculations: for the  $n_{corr} = 30$  horizontal and vertical dipole correctors with the maximal strength of  $\theta_{corr} \leq 0.5$  mrad and located in the ring more or less uniformly, the orbit distortions could be minimized to the

required values taking to the account the technically realized tolerances for dipole guiding field and quadrupole alignment. The excursions of the uncorrected closed orbits are shown in Fig. 4 and the required corrector kicks distributions are shown in Fig. 5.

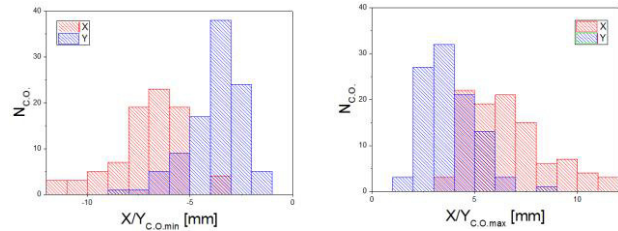


Figure 4: Closed orbit distortion statistics for 100 random orbits. Maximal/minimal pick-up reading before correction.

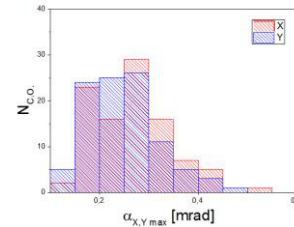


Figure 5: Maximal values of horizontal/vertical dipole corrector strength for the required residual orbit of  $\sigma_{x/y} = 0.1$  mm.  $n_{corr} = 30$ ,  $\theta_{corr,max} = 0.5$  mrad,  $B_{corr,max} = 0.15$  T.

The correction of the linear betatron tunes  $Q_{x,y}$  is produced by the structural quadrupole lenses. For example, the move from the first working point  $Q_{x,y} = 9.44/9.44$  (Fig. 6) to the second one  $Q_{x,y} = 9.10/9.10$  is produced by current correction -300 A in all quadrupole, except final focus quadrupoles, and +9 A in QD arc quadrupoles.

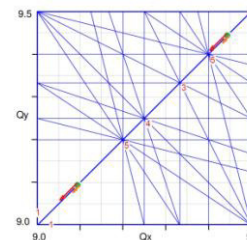


Figure 6: Resonance diagram up to 5<sup>th</sup> order. Collider working points of betatron tunes. Space charge tune shifts at 1 and 4.5 GeV/u.

The skew quadrupole correctors are used in collider optics for two reasons: correction of betatron coupling and local correction of the vertical dispersion. The first problem supposes four families (independent current supplies) placed in straight sections. Taking into account the main sources of coupling in the collider rings, MPD detector solenoid (5.8 m long,  $B_{s,max} = 0.5$  T), electron cooler solenoid (6 m long,  $B_{s,max} = 0.2$  T), the required maximal gradient of the skew quadrupole winding is about 2.5 T/m in the worst case of one direction of the solenoid fields. Due to the vertical separation of the beams there is the small uncorrected vertical dispersion in

the collider rings. The local suppression of the vertical dispersion  $D_y$  requires two additional skew quadrupole families located in the bending arcs next to  $D_x$  maximum.

The correction of the chromaticity of betatron tunes is the principal task in the collider because the large natural chromaticities of  $Q'_{x,y} \approx -30$  due to the large variation of the  $\beta$ -functions in the ring especially in the beam separation and interaction regions. System of the chromaticity correction includes 4 families of sextupole correctors (focusing and defocusing) placed near focusing and defocusing quadrupoles in the arcs. Sextupoles in each family are sit apart in  $180^\circ$  betatron phase advance for the compensation of their nonlinear influence on the dynamic aperture (DA). The dependence of the collider tune on  $\Delta p/p$  is shown in Fig. 7 before and after chromaticity correction (maximum sextupole strength of  $150 \text{ T/m}^2$  at the maximum energy of  $4.5 \text{ GeV/u}$ ). The value of the sextupole harmonics of the dipole field expected from the magnetic measurements is about  $b_3=5 \cdot 10^{-4}$  ( $r=30 \text{ mm}$ ) at the highest energy of  $E_k=4.5 \text{ GeV/u}$ . This nonlinear component of the field changes the chromaticities and increase the maximal corrector strength of the defocusing family up to the  $175 \text{ T/m}^2$ .

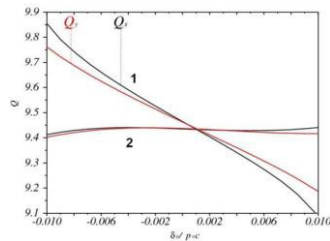


Figure 7: Tune spread over the momentum acceptance before (1) and after (2) chromaticity correction.

The collider dynamic aperture (DA) calculations [2] were carried out with the possible nonlinearities of the magnetic field. The proper harmonics of the structural dipole and quadrupole magnets introduce the small influence on DA. The chromaticity correction operates anytime of particle tracking. The fringe fields of the magnetic elements, in particular, the final focus quadrupoles, show the most severe effect on the collider DA. Following the dependence of the fringe field kick in quadrupole  $\Delta\theta/\theta \sim \beta^2 \cdot k^2 \cdot d \cdot \epsilon$ , this effect could be reduced by the decreasing the beta-function  $\beta$  in quadrupole, quadrupole strength  $k$  and length  $d$ , and also the beam emittance  $\epsilon$ . In the case of the final focus quadrupoles increasing the  $\beta^*$  in IP decreases the maximal value of  $\beta$ -function in quadrupole and decreases the fringe field effect. The DA calculations by MAD-X [3] include the fringe field in all magnetic elements. The correction of this influence on DA by the linear arrangement of the collider optics is shown in Fig. 8, where the stable DAs in the terms of beam amplitude are given for the  $\beta^*=0.35 \text{ m}$  and  $\beta^*=0.60 \text{ m}$ . Optics with the  $\beta^*=0.60 \text{ m}$  in IP provides the double excess of DA over the geometrical acceptance. This optics needs the beam intensity increase due to 25% drop of luminosity.

The DA increase by introduction of the octupole nonlinearities is carried out. The additional octupole windings near final focus quadrupoles (two families with gradients of  $60$  and  $150 \text{ T/m}^3$ ) could improve the situation (Fig. 9).

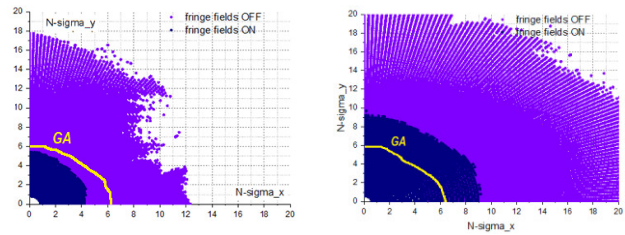


Figure 8: Collider DA in terms of beam amplitude.  $q_{x,y}=0.44$ ,  $\beta^*=0.35\text{m}$  (left),  $0.6\text{m}$  (right). GA – geometrical acceptance.

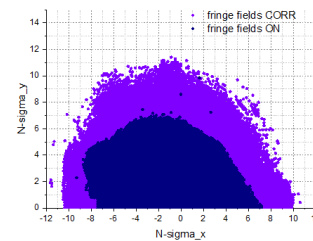


Figure 9: Collider DA with fringe field switch-on and octupole correction effect.

Идентификационный номер		Положение катушки	
SPB	№ катушки	№ катушки	SPB
bl	MCA1	MCA2	MCA3
bl	MCA4	MCA5	MCA6
bl	MCA7	MCA8	MCA9
bl	MCA10	MCA11	MCA12
bl	MCA13	MCA14	MCA15
bl	MCA16	MCA17	MCA18
bl	MCA19	MCA20	MCA21
bl	MCA22	MCA23	MCA24
bl	MCA25	MCA26	MCA27
bl	MCA28	MCA29	MCA30
bl	MCA31	MCA32	MCA33
bl	MCA34	MCA35	MCA36
bl	MCA37	MCA38	MCA39
bl	MCA40	MCA41	MCA42
bl	MCA43	MCA44	MCA45
bl	MCA46	MCA47	MCA48
bl	MCA49	MCA50	MCA51
bl	MCA52	MCA53	MCA54
bl	MCA55	MCA56	MCA57
bl	MCA58	MCA59	MCA60
bl	MCA61	MCA62	MCA63
bl	MCA64	MCA65	MCA66
bl	MCA67	MCA68	MCA69
bl	MCA70	MCA71	MCA72
bl	MCA73	MCA74	MCA75
bl	MCA76	MCA77	MCA78
bl	MCA79	MCA80	MCA81
bl	MCA82	MCA83	MCA84
bl	MCA85	MCA86	MCA87
bl	MCA88	MCA89	MCA90
bl	MCA91	MCA92	MCA93
bl	MCA94	MCA95	MCA96
bl	MCA97	MCA98	MCA99
bl	MCA100	MCA101	MCA102
bl	MCA103	MCA104	MCA105
bl	MCA106	MCA107	MCA108
bl	MCA109	MCA110	MCA111
bl	MCA112	MCA113	MCA114
bl	MCA115	MCA116	MCA117
bl	MCA118	MCA119	MCA120
bl	MCA121	MCA122	MCA123
bl	MCA124	MCA125	MCA126
bl	MCA127	MCA128	MCA129
bl	MCA130	MCA131	MCA132
bl	MCA133	MCA134	MCA135
bl	MCA136	MCA137	MCA138
bl	MCA139	MCA140	MCA141
bl	MCA142	MCA143	MCA144
bl	MCA145	MCA146	MCA147
bl	MCA148	MCA149	MCA150
bl	MCA151	MCA152	MCA153
bl	MCA154	MCA155	MCA156
bl	MCA157	MCA158	MCA159
bl	MCA160	MCA161	MCA162
bl	MCA163	MCA164	MCA165
bl	MCA166	MCA167	MCA168
bl	MCA169	MCA170	MCA171
bl	MCA172	MCA173	MCA174
bl	MCA175	MCA176	MCA177
bl	MCA178	MCA179	MCA180
bl	MCA181	MCA182	MCA183
bl	MCA184	MCA185	MCA186
bl	MCA187	MCA188	MCA189
bl	MCA190	MCA191	MCA192
bl	MCA193	MCA194	MCA195
bl	MCA196	MCA197	MCA198
bl	MCA199	MCA200	MCA201
bl	MCA202	MCA203	MCA204
bl	MCA205	MCA206	MCA207
bl	MCA208	MCA209	MCA210
bl	MCA211	MCA212	MCA213
bl	MCA214	MCA215	MCA216
bl	MCA217	MCA218	MCA219
bl	MCA220	MCA221	MCA222
bl	MCA223	MCA224	MCA225
bl	MCA226	MCA227	MCA228
bl	MCA229	MCA230	MCA231
bl	MCA232	MCA233	MCA234
bl	MCA235	MCA236	MCA237
bl	MCA238	MCA239	MCA240
bl	MCA241	MCA242	MCA243
bl	MCA244	MCA245	MCA246
bl	MCA247	MCA248	MCA249
bl	MCA250	MCA251	MCA252
bl	MCA253	MCA254	MCA255
bl	MCA256	MCA257	MCA258
bl	MCA259	MCA260	MCA261
bl	MCA262	MCA263	MCA264
bl	MCA265	MCA266	MCA267
bl	MCA268	MCA269	MCA270
bl	MCA271	MCA272	MCA273
bl	MCA274	MCA275	MCA276
bl	MCA277	MCA278	MCA279
bl	MCA280	MCA281	MCA282
bl	MCA283	MCA284	MCA285
bl	MCA286	MCA287	MCA288
bl	MCA289	MCA290	MCA291
bl	MCA292	MCA293	MCA294
bl	MCA295	MCA296	MCA297
bl	MCA298	MCA299	MCA300
bl	MCA301	MCA302	MCA303
bl	MCA304	MCA305	MCA306
bl	MCA307	MCA308	MCA309
bl	MCA310	MCA311	MCA312
bl	MCA313	MCA314	MCA315
bl	MCA316	MCA317	MCA318
bl	MCA319	MCA320	MCA321
bl	MCA322	MCA323	MCA324
bl	MCA325	MCA326	MCA327
bl	MCA328	MCA329	MCA330
bl	MCA331	MCA332	MCA333
bl	MCA334	MCA335	MCA336
bl	MCA337	MCA338	MCA339
bl	MCA340	MCA341	MCA342
bl	MCA343	MCA344	MCA345
bl	MCA346	MCA347	MCA348
bl	MCA349	MCA350	MCA351
bl	MCA352	MCA353	MCA354
bl	MCA355	MCA356	MCA357
bl	MCA358	MCA359	MCA360
bl	MCA361	MCA362	MCA363
bl	MCA364	MCA365	MCA366
bl	MCA367	MCA368	MCA369
bl	MCA370	MCA371	MCA372
bl	MCA373	MCA374	MCA375
bl	MCA376	MCA377	MCA378
bl	MCA379	MCA380	MCA381
bl	MCA382	MCA383	MCA384
bl	MCA385	MCA386	MCA387
bl	MCA388	MCA389	MCA390
bl	MCA391	MCA392	MCA393
bl	MCA394	MCA395	MCA396
bl	MCA397	MCA398	MCA399
bl	MCA400	MCA401	MCA402
bl	MCA403	MCA404	MCA405
bl	MCA406	MCA407	MCA408
bl	MCA409	MCA410	MCA411
bl	MCA412	MCA413	MCA414
bl	MCA415	MCA416	MCA417
bl	MCA418	MCA419	MCA420
bl	MCA421	MCA422	MCA423
bl	MCA424	MCA425	MCA426
bl	MCA427	MCA428	MCA429
bl	MCA430	MCA431	MCA432
bl	MCA433	MCA434	MCA435
bl	MCA436	MCA437	MCA438
bl	MCA439	MCA440	MCA441
bl	MCA442	MCA443	MCA444
bl	MCA445	MCA446	MCA447
bl	MCA448	MCA449	MCA450
bl	MCA451	MCA452	MCA453
bl	MCA454	MCA455	MCA456
bl	MCA457	MCA458	MCA459
bl	MCA460	MCA461	MCA462
bl	MCA463	MCA464	MCA465
bl	MCA466	MCA467	MCA468
bl	MCA469	MCA470	MCA471
bl	MCA472	MCA473	MCA474
bl	MCA475	MCA476	MCA477
bl	MCA478	MCA479	MCA480
bl	MCA481	MCA482	MCA483
bl	MCA484	MCA485	MCA486
bl	MCA487	MCA488	MCA489
bl	MCA490	MCA491	MCA492
bl	MCA493	MCA494	MCA495
bl	MCA496	MCA497	MCA498
bl	MCA499	MCA500	MCA501
bl	MCA502	MCA503	MCA504
bl	MCA505	MCA506	MCA507
bl	MCA508	MCA509	MCA510
bl	MCA511	MCA512	MCA513
bl	MCA514	MCA515	MCA516
bl	MCA517	MCA518	MCA519
bl	MCA520	MCA521	MCA522
bl	MCA523	MCA524	MCA525
bl	MCA526	MCA527	MCA528
bl	MCA529	MCA530	MCA531
bl	MCA532	MCA533	MCA534
bl	MCA535	MCA536	MCA537
bl	MCA538	MCA539	MCA540
bl	MCA541	MCA542	MCA543
bl	MCA544	MCA545	MCA546
bl	MCA547	MCA548	MCA549
bl	MCA550	MCA551	MCA552
bl	MCA553	MCA554	MCA555
bl	MCA556	MCA557	MCA558
bl	MCA559	MCA560	MCA561
bl	MCA562	MCA563	MCA564
bl	MCA565	MCA566	MCA567
bl	MCA568	MCA569	MCA570
bl	MCA571	MCA572	MCA573
bl	MCA574	MCA575	MCA576
bl	MCA577	MCA578	MCA579
bl	MCA580	MCA581	MCA582
bl	MCA583	MCA584	MCA585
bl	MCA586	MCA587	MCA588
bl	MCA589	MCA590	MCA591
bl	MCA592	MCA593	MCA594
bl	MCA595	MCA596	MCA597
bl	MCA598	MCA599	MCA600
bl	MCA601	MCA602	MCA603
bl	MCA604	MCA605	MCA606
bl	MCA607	MCA608	MCA609
bl	MCA610	MCA611	MCA612
bl	MCA613	MCA614	MCA615
bl	MCA616	MCA617	MCA618
bl	MCA619	MCA620	MCA621
bl	MCA622	MCA623	MCA624
bl	MCA625	MCA626	MCA627
bl	MCA628	MCA629	MCA630
bl	MCA631	MCA632	MCA633
bl	MCA634	MCA635	MCA636
bl	MCA637	MCA638	MCA639
bl	MCA640	MCA641	MCA642
bl	MCA643	MCA644	MCA645
bl	MCA646	MCA647	MCA648
bl	MCA649	MCA650	MCA651
bl	MCA652	MCA653	MCA654
bl	MCA655	MCA656	MCA657
bl	MCA658	MCA659	MCA660
bl	MCA661	MCA662	MCA663
bl	MCA664	MCA665	MCA666
bl	MCA667	MCA668	MCA669
bl	MCA670	MCA671	MCA672
bl	MCA673	MCA674	MCA675
bl	MCA676	MCA677	MCA678
bl	MCA679	MCA680	MCA681
bl	MCA682	MCA683	MCA684
bl	MCA685	MCA686	MCA687
bl	MCA688	MCA689	MCA690
bl	MCA691	MCA692	MCA693
bl	MCA694	MCA695	MCA696
bl	MCA697	MCA698	MCA699
bl	MCA700	MCA701	MCA702
bl	MCA703	MCA704	MCA705
bl	MCA706	MCA707	MCA708
bl	MCA709	MCA710	MCA711
bl	MCA712	MCA713	MCA714
bl	MCA715	MCA716	MCA717
bl	MCA718	MCA719	MCA720
bl	MCA721	MCA722	MCA723
bl	MCA724	MCA725	MCA726
bl			